www.amlett.org, www.amlett.com, DOI: 10.5185/amlett.2012.5354 Published online by the VBRI press in 2012

Polyamide 66/nanoclay composites: Synthesis, thermal and flammability properties

Sudesh Rathi and J. B. Dahiya*

Department of Chemistry, G. J. University of Science & Technology, Hisar 125001, Haryana, India

*Corresponding author. Tel.: (+91) 1662-263356; Fax: (+91) 1662-276240; E-mail: jbdic@yahoo.com

Received: 23 May 2012, Revised: 17 June 2012, Accepted: 20 June 2012

ABSTRACT

PA66/nanoclay nanocomposites with flame retardant (dimelamine phosphate) and other supportive additives (ammonium pentaborate, zinc borate and potassium nitrate) were prepared by melt blending method using single screw extruder. The prepared nanocomposites were characterized by XRD and FTIR techniques. The thermal properties were analysed using thermogravimetry and differential scanning calorimetry. A significant reduction in flame spread rate in UL-94 horizontal test was observed on inclusion of ammonium pentaborate to PA66/nanoclay/dimelamine phosphate composite. Copyright © 2012 VBRI Press.

Keywords: Poyamide 66; nanoclay; thermogravimetry; thermal stability; UL-94 test.

Sudesh Rathi is pursuing Ph.D. from Department of Chemistry, G. J. University of Science and Technology, Hisar (Haryana), India under the supervision of Prof. J. B. Dahiya. She has been awarded Junior Research fellowship (JRF) by Council of Scientific and Industrial Research (CSIR), New Delhi, to carry out research work. She has published and presented four papers in journals and conferences. She is working in the area of flame retardancy of polymeric materials.

J. B. Dahiya received Ph.D. degree in 1991 from Kurukshetra University, Kurukshetra, India. He joined Department of Chemistry, G. J. University of Science and Technology, Hisar, India as Assistant Professor in 1995 and became Professor in 2009. He has published over 30 papers in journals and conferences. He visited Germany twice on DAAD fellowship in 2004 and 2008. He visited UK in 2010-11 on Commonwealth Academic Staff Fellowship. His major research interest includes flame retardant polymers.

Introduction

Synthetic polymeric materials provide numerous advantages in everyday life. But there is a major disadvantage related to high flammability of such materials being organic in nature and limits their wider applications. To increase the applications of polymers, a major challenge for recent research is to enhance the fire retardant and heat resistance properties of polymers [**1**]. Nanocomposites are a new class of composites, for which at least one dimension of the added particles, is in the nanometer range. Nanocomposites are generally organic polymer composites with inorganic nanoscale dispersed particles which leads to a dramatic increase in interfacial area as compared with traditional composites. They combine the advantages of the inorganic material (e.g., rigidity, thermal stability) and the organic polymer (e.g., flexibility, dielectric, ductility, and processability). Generally, inclusion of clay particles enhance the thermal stability of polymers by acting as thermal insulator [**2**] and mass transport barrier [**3**] to the volatile products generated during decomposition. However, it is very difficult for the hydrophilic clay (montmorrilonite) to be exfoliated and well-dispersed in a hydrophobic polymer matrix. Therefore, organically modified clay (nanoclay) is generally used with objective to expand the interlayer space of the clay and allowing large polymer molecules to enter into the interlayer space. Melt intercalation is most commonly used solvent less approach to synthesize polymer/clay nanocomposites. Melt intercalation method involves diffusion of the polymer chains into the space between the clay and the galleries.

Table 1. Composition of PA66/NM composites and major DTA peaks.

Sample	Composition (%)	DTA Temperature (°C)		Nature of peak
		Initiation	*Maximum*	
PA66	100	245	262	Endo
		360	425	Endo
PA66/NM	95+5	206	262	Endo
		322	447	Endo
PA66/NM/DMP	80+5+15	250	260	Endo
		326	383	Endo
PA66/NM/DMP/APB	80+5+10+5	246	262	Endo
		340	410	Endo
PA66/NM/DMP/APB/ZB	80+5+10+2.5+2.5	205	262	Endo
		335	409	Endo
PA66/NM/DMP/APB/KN	80+5+10+2.5+2.5	242	260	Endo
		334	404	Endo

Conventional flame retardants are required in large quantity to make the polymer fire rertardant which may affect the processing of polymer. By use of organically modified clay (nanoclay), interaction between the clay particles and the polymer matrix has been enhanced [**4, 5**]. Polymer/nanoclay composites are considered a radical alternative to conventionally filled polymers. Most of the mechanical properties are found increased on inclusion of nanoclays to polymers but generally do not pass commercial flammability tests. So, a combined approach of nanoclay and conventional flame retardants is studied in the present work.

Polyamide 66 (PA66) is a semicrystalline engineering thermoplastic commodity polymer that finds widespread use in various applications. Recently much attention has been focussed on PA66/organoclay nanocomposites preparation by melt blending method [**6, 7**], which is a solvent free approach and industrial viable to synthesize polymer-clay nanocomposite and broadly applicable to many polar and nonpolar polymers.

In this study, composites of PA66 and nanoclay along with some conventional additives such as dimelamine phosphate (DMP), ammonium pentaborate (APB), zinc borate (ZB) and potassium nitrate (KN) were prepared by melt blending method. The composites were characterized by x-ray diffraction (XRD) and Fourier Transform Infrared Spectroscopy (FTIR). The thermal and flammable behaviour of the composites was investigated through thermogravimetry, differential scanning calorimetry and UL-94 test

Experimental

Materials

Polyamide 66 and nanoclay (Nanomer 1.34 TCN, i.e., natural montmorillonite modified with methyl tallow bis−(2−hydroxyethyl) hydrogenated quaternary ammonium cation) were purchased from Sigma Aldrich Co., India. The nanoclay is represented as NM in this study. The additives such as dimelamine phosphate (DMP), zinc borate (ZB) and potassium nitrate (KN) were purchased from Himedia Chemicals Co., India. Ammonium pentaborate (APB) was purchased from S-d fine Chemicals Co., India. All these materials were used without further purification. The composition of various PA66/nanoclay composites is given in **Table 1**.

Preparation of PA66/nanoclay composites

PA66, nanoclay and other additives with desired proportions (**Table 1**) was melt blended using single screw extruder (Maxwell mixing extruder, ¾ inch dia.) with a feed rate of 200 g/h to yield the composites. Prior to extrusion, PA66 pellets were oven dried at 85 °C for 10 h and grinded to obtain coarse material. Extrusion was performed within the temperature range 240−250 °C at a screw speed of 30 rpm. The strands obtained from extruder were palletized using the pinch rolls of the Take up (CS−194T) and chopper (CS−194C) which was again oven dried at 80 °C for 10 h and grinded to be used for further analysis.

Characterization

X-ray diffraction (XRD) measurements were performed with RIGAKU MINIFLEX- II equipped with a Cu−Kα radiation (λ = 0.1542 nm, 30 kV, 15 mA) with 2θ scan range of 3−30° at room temperature. Thermal analysis (TG-DTA) was performed at a heating rate of 10 °C/min from ambient temperature to 700 °C in nitrogen atmosphere (flow rate = 100 mL/min) using TA instruments Q600 SDT. Differential scanning calorimetry (DSC) analysis was carried out using a TA instruments DSC Q−10 thermal analyzer from 40 to 500 °C at a heating rate of 10 °C/min under constant nitrogen flow of 50 mL/min. For testing the flammability of samples, UL-94 test was carried out in horizontal and vertical modes according to ISO 1210. In this test, the test samples in form of strands marked at a length of 100 mm were used. The Bunsen flame of controlled intensity was applied and the time taken to reach the flame to 100 mm mark was measured. The results reported are the average of three replicated experiments. Infrared spectra of PA66 and its composites were recorded at room temperature with Shimadzu IR affinity-I 8000 FTIR spectrophotometer in the wavenumber range from 4000 to 400 cm^{-1} for 15 scans with a resolution of 4 cm^{-1}. The PA66/nanoclay composite samples were also heated in

a furnace at 400 °C for 10 min to observe the swelling and charring behaviour while heating.

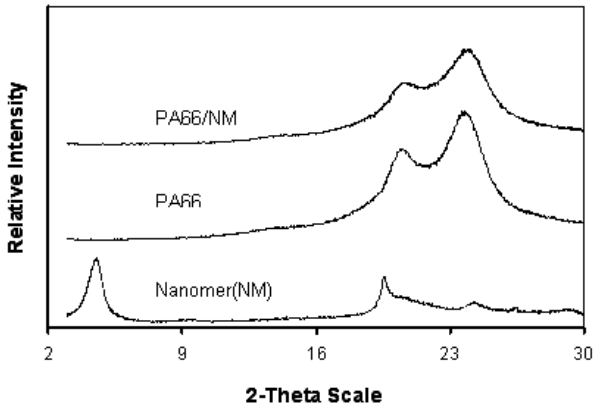

Fig. 1. XRD pattern of nanomer (NM), PA66 and PA66/NM composite.

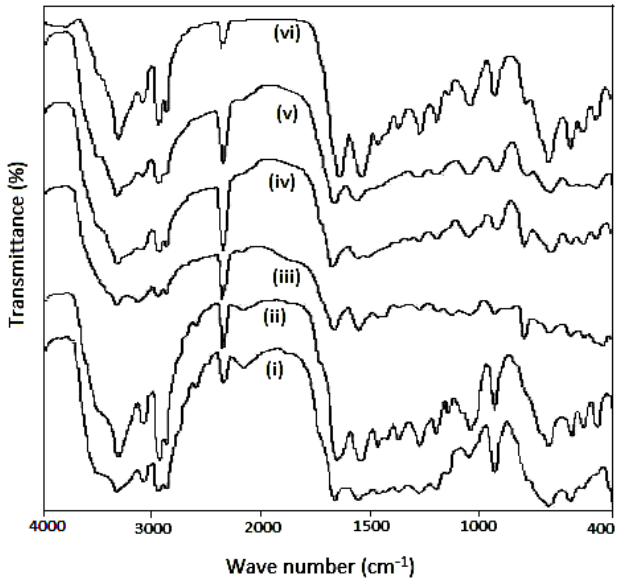

Fig. 2. Infrared spectra of (i) PA66, (ii) PA66/NM, (iii) PA66/NM/DMP, (iv) PA66/NM/DMP/APB, (v) PA66/NM/DMP/APB/ZB and (vi) PA66/NM/DMP/APB/KN.

Results and discussion

XRD spectra

Fig. 1 shows the XRD pattern of PA66, nanoclay (NM) and PA66/NM composite. Polymer/clay nanocomposites are formed by insertion of polymer chains between the clay layers with increased gallery space. A shift in d_{001} peak of clay in XRD spectrum is associated with the formation of an intercalated structure, while disappearance of this peak is indicative of an exfoliated structure in nanocomposites. The basal spacing of NM was found 1.78 nm corresponding to $2\theta = 4.94^o$. For PA66/NM composite, the characteristic peak of NM is absent up to the angle of 3^o which suggests that the NM has nearly exfoliated effect in the PA66 matrix.

The XRD curve of neat PA66 exhibits two intense and well resolved peaks at $2\theta = 20^o$ (α1) and 24^o (α2) at room temperature confirming α form of PA66 [**8**]. These diffraction peaks are assigned to (100) and (010, 110) crystal planes, respectively [**9**]. The alpha form of PA66 at room temperature is thermodynamically more stable than that of PA6. Therefore, crystalline transformations are less feasible in PA66/NM nanocomposites. PA66 has various crystalline phases and usually presents the more stable α phase rather than the γ phase in XRD pattern. The incorporation of nanoclay in PA66 shows slight reduction in the relative intensities of α1 and α2 peaks.

Infrared studies of PA66/nanomer composites

FTIR spectra are used in this study as a qualitative measurement to analyze the chemical structure of all the samples. The FTIR spectra of pure PA66, nanomer and their composites are presented in **Fig. 2**. The major peaks associated with pure PA66 are hydrogen-bonded N—H stretching at 3319 cm^{-1}, N—H bending overtone at 3076 cm^{-1}, asymmetric CH_2 stretching at 2943 cm^{-1}, symmetric CH_2 stretching at 2866 cm^{-1}, C═O stretching (amide I) at 1663 cm^{-1}, in−plane N—H bending (amide II) at 1558 cm^{-1}, CH_2 symmetric bending at 1468 cm^{-1}, CH_2 symmetric bending (CH_2 next to N) at 1435 cm^{-1}, C—N stretching (amide III) at 1277 cm^{-1}, α-phase of PA66 at 933 cm^{-1}, out-of-plane N—H bending (amide V) at 685 cm^{-1} and OCN bending (amide VI) at 584 cm^{-1} [**10,11**]. The clay (NM) sample shows the following peaks: sharp peak at 3636 cm^{-1} due to —OH stretching for Al—OH and Si—OH , broad peak at 3379 cm^{-1} due to —OH stretching of interlayer water, sharp peak at 1639 cm^{-1} due to —OH bending mode in adsorbed water, small peak at 1111 cm^{-1} due to out of plane Si—O stretching, small peaks at 920, 885 and 847 cm^{-1} due to AlAlOH, AlFeOH and AlMgOH bending and small peak at 520 cm^{-1} due to Si—O bending of NM [**12-14**].

The increase in intensity of the band at 1663 cm^{-1} is found in case of PA66/NM composite which corresponds to the carbonyl group. The peak at 1438 cm^{-1} in case of PA66/NM/DMP/APB shows B—O stretching of APB which gets diminished in PA66/NM/DMP/APB/ZB and PA66/NM/DMP/APB/KN composites as the loading of APB is decreased from 5 to 2.5 wt%. In case of PA66/NM/DMP, the peaks in the range of 1100-1275 cm^{-1} corresponds to P═O stretching.

In case of PA66/NM/DMP/APB/KN, the intensities of the peaks at 1541 and 1641 cm^{-1} are found to be increased and an additional peak at 1371 cm^{-1} shows the presence of NO_3^- ion alongwith the peaks of PA66, NM, DMP and APB.

Thermal analysis

The thermal parameters of various PA66 composites with clay and additives (PA66, PA66/NM, PA66/NM/DMP, PA66/NM/DMP/APB, PA66/NM/DMP/APB/ZB and PA66/NM/DMP/APB/KN) were obtained from their TG curves (**Fig. 3** and **4**) and are given in **Table 2**. The parameters used for comparing thermal stability are the onset degradation temperature, $T_{10wt\%}$, (temperature at 10% mass loss), mid-point temperature, $T_{50wt\%}$ (temperature at 50% mass loss) and the residual mass i.e. char at 600 °C.

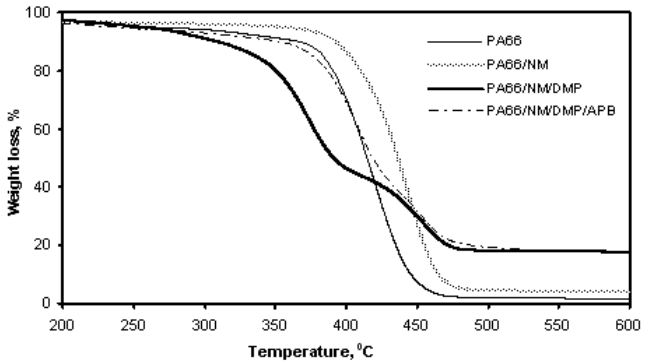

Fig. 3. TG curves of PA66, PA66/NM, PA66/NM/DMP and PA66/NM/DMP/APB composites.

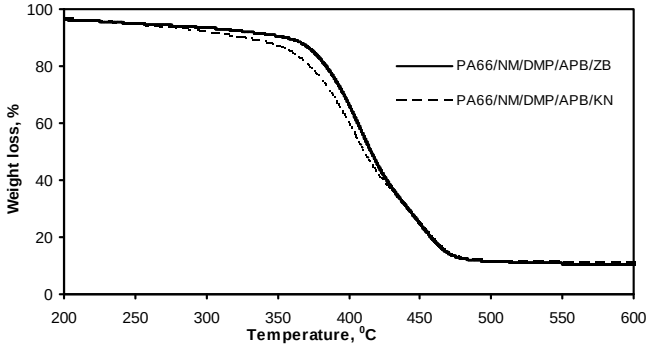

Fig. 4. TG curves of PA66/NM/DMP/APB/ZB and PA66/NM/DMP/APB/KN composites.

From TG curve (**Fig. 3)**, the thermal degradation behaviour of PA66 is observed in two stages. The onset degradation temperature of PA66 is found to be 367 ^{o}C. The minor weight loss during first stage from PA66 polymer is attributed to absorbed water, unreacted monomer and light volatile oligomers. During second stage, the major weight loss of PA66 is observed in the temperature range 360-500 ^{o}C and this weight loss is due to certain decomposition reactions with endothermic maximum at 425 ^{o}C in DTA curve (**Table 1**). PA66 decomposes via primary polyamide chain scission, hydrolysis, homolytic chain scission, intramolecular C—H transfer and cis elimination producing mostly linear or cyclic oligomeric fragments and monomeric units [**15-17**]. After this main step of PA66 degradation, the degradation process of aromatized and intermediate crosslinked products becomes slow leaving a stable char residue of 1.5 wt % at 600 ^{o}C.

On inclusion of 5 wt % NM to pure PA66, the $T_{10wt\%}$ and $T_{50wt\%}$ are found increased by 25 and 21 ^{o}C respectively, which shows that PA66 containing nanomer (NM) presents superior thermal stability than PA66 due to formation of nanocomposite. The maximum of endothermic peak (447 ^{o}C) in DTA curve is also increased by 22 ^{o}C. Generally the organoclay affects thermal stability of the nanocomposites by two ways, one is due to barrier property to the oxygen increasing the stability and the other is due to the catalysis effect toward the degradation of the polymer. In this study, the barrier effect is predominant as the fraction of clay added to the polymer matrix is low. Araujo et al. [**18**] and Zhao et al. [**19**] also reported that the catalyzing effect becomes dominant only with increasing loading of clay and the thermal stability of the nanocomposites decreases. In polyamide/layered silicate nanocomposite, the flame resistance is probably provided by producing a unique kind of char after burning between the layers of silicates.

The addition of DMP to PA66/NM initially destabilises the composite most in this study since both $T_{10wt\%}$ and $T_{50wt\%}$ are decreased by 84 and 45 ^{o}C in comparison to that of pure PA66/NM. The PA66/NM/DMP composite, shows an extra stage of thermal degradation between 287 and 404 ^{0}C due to the evaporation of melamine on decomposition of DMP [**20**]. The mass loss rate slows down after 404 ^{0}C giving rise to comparatively higher carbonaceous silicate char residue (17.9 %) at 600 ^{0}C, which insulates the underlying material as well as reduces the volatile decomposition products [**21**], and hence increasing the thermal stability of nanocomposite at higher temperature. There is a strong correlation between char yield and fire resistance as the char is formed at the expense of combustible gases and the presence of a char inhibits further flame spread by acting as a thermal barrier around the unburned material. It has been shown previously by Levchik et al [**22**] that the mechanism of the fire retardant action of dimelamine phosphate is similar to the ammonium polyphosphate, since melamine, by analogy with ammonia volatilizes, whereas the remaining phosphoric acids produce esters with nylon 6, which are precursors of the char.

On addition of APB to PA66/NM/DMP, the onset degradation temperature and mid-point temperature are found to be increased by 40 and 27 ^{o}C respectively. The TG curve of PA66/NM/DMP/APB (**Fig. 3**) shows weight loss in the temperature range 100-230 ^{o}C due to thermal decomposition of APB. The dehydration of APB takes place at higher temperature (230-450 ^{o}C) producing ammonia and pentaboric acid which in due course converted to a boric oxide glass [**23**]. The pentaboric acid released from APB initially catalyses the degrdation of the PA66/NM/DMP but later on the composite becomes thermally stable as a molten glassy layer of boric acid/boric anhydride is accumulated on the surface of burning polymer creating a barrier against diffusion of the volatile fuel from the polymer to the flame, which decreases combustibility of PA66.

When 2.5 wt % APB out of total 5 wt % is replaced by 2.5 wt% ZB for PA66/NM/DMP/APB/ZB, no significant changes in onset temperature of degradation is observed but stability after 420 ^{o}C as well as char at 600 ^{o}C are decreased may be due to formation of thin glassy layer at surface. In case of PA66/NM/DMP/APB/KN composite no improvement in stability and char yield is observed.

Char yield

Table 2 shows almost negligible residue for pure PA66 at 600 ^{o}C. The increased char yield in case of PA66/NM (4.3%) is observed due to presence of nondegradable clay moiety. The char yield of PA66/NM/DMP and PA66/NM/DMP/APB increases to 17.1—17.9% at 600 ^{o}C due to presence of DMP. The increase in observed char

Table 2. TG data of PA66/NM composites under nitrogen flow.

Sample	Stage	Temp. range (^{o}C)	Wt. Loss (%)	$T_{10wt\%}$ (^{o}C)	$T_{50wt\%}$ (^{o}C)	Char at 600 ^{0}C (%)	
						Observed	*Calculated*
PA66	1st	100-360	6.83	367	415	1.5	--
	2nd	360-700	89.29				
PA66/NM	1st	100-354	3.2	392	436	4.3	4.4
	2nd	354-700	90.6				
PA66/NM/DMP	1st	100-287	7.53	308	391	17.9	7.5
	2nd	287-404	47.04				
	3rd	404-700	27.67				
PA66/NM/DMP/APB	1st	100-333	6.7	348	418	17.1	9.5
	2nd	333-700	74.7				
PA66/NM/DMP/APB/ZB	1st	100-339	7.0	356	415	10.3	9.9
	2nd	339-700	81.6				
PA66/NM/DMP/APB/KN	1st	100-331	8.3	324	410	11.1	10.3
	2nd	331-700	78.6				

Table 3. Characteristic values of DSC measurements of PA66/NM composites under nitrogen flow.

Samples	DSC temperature (^{o}C)		Heat flow (J/g)	Nature of peak
	Initiation	*Maximum*		
PA66	250	261	75	Endo
	391	446	594	Endo
PA66/NM	252	261	74	Endo
	396	446	454	Endo
PA66/NM/DMP	250	261	61	Endo
	284	299	16	Endo
	344	384	275	Endo
	454	459	28	Endo
PA66/NM/DMP/APB	210	230	10	Endo
	252	262	43	Endo
	377	407	315	Endo
PA66/NM/DMP/APB/ZB	250	262	79	Endo
	376	415	278	Endo
PA66/NM/DMP/APB/KN	248	260	52	Endo
	356	371	42	Endo
	376	410	54	Endo

yield is actually higher than the calculated char yield on the basis of individual contributions of PA66, NM, DMP and APB to the residue indicating that more effective carbonizing and cross linking process takes place on addition of DMP. Negligible contribution on addition of ZB and KN to PA66 composites is observed towards char formation.

DSC studies of PA66/nanomer composites

DSC thermograms of PA66/NM composites are shown in **Fig. 5**. The initiation and maximum temperatures alongwith heat flow and nature of DSC peaks are given in **Table 3**. DSC curve of pure PA66 shows first endotherm with maximum at 260 ^{o}C which is due to the melting point of PA66. The PA66 gives one more endotherm at 446 ^{o}C with heat absorption value of 594 J/g corresponding to the major thermal degradation of pure PA66. On addition of NM to PA66, similar DSC curve is obtained. No change in melting point of PA66 polymer is observed on formation of nanocomposite and also the major thermal degradation peak is observed at same temperature i.e. 446 ^{o}C but with lower heat of absorption (454 J/g). PA66/NM/DMP and PA66/NM/DMP/APB samples show major endotherms at 384 and 407 ^{o}C with 275 and 315 J/g heat absorption values, respectively, due to decomposition. PA66/NM/DMP/APB composite shows an additional peak

before melting at 230 °C which may be due to early decomposition of APB. The results of TG and DSC show that addition of DMP and APB to PA66/NM nanocomposite increases the char formation capacity of the nanocomposites thus increasing the fire resistance property.

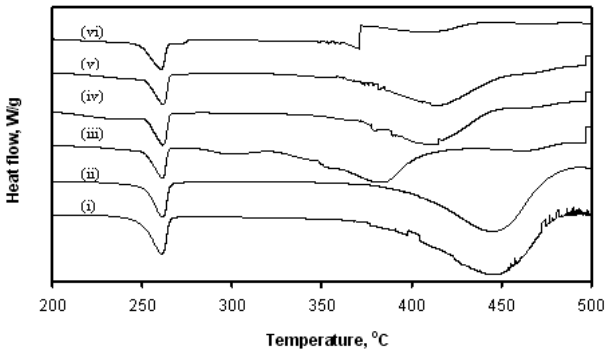

Fig. 5. DSC spectra of (i) PA66, (ii) PA66/NM, (iii) PA66/NM/DMP, (iv) PA66/NM/DMP/APB, (v) PA66/NM/DMP/APB/ZB and (vi) PA66/NM/DMP/APB/KN.

Fig. 6. Digital photographs of residues after heating at 400 °C of (i) PA66, (ii) PA66/NM and (iii) PA66/NM/DMP.

Table 4. UL-94 test data for PA66/NM composites.

Sample	t (sec)	Number of drips	Flame spread rate (mm/sec)	UL-94 rating
PA66	69	37	1.45	NR
PA66/NM	48	5	2.08	NR
PA66/NM/DMP	78	2	1.28	NR
PA66/NM/DMP/APB	172	3	0.58	NR
PA66/NM/DMP/APB/ZB	70	2	1.43	NR
PA66/NM/DMP/APB/KN	68	2	1.47	NR

t: time to burn up to 100 mm, NR: no rating.

Residue morphology

PA66 and PA66/NM composites were heated in a muffle furnace for about 10 minutes and the images of residue obtained are shown in **Fig. 6.** A continuous and compact char layer as an over coat is seen on the surface of PA66/NM composite which may delay the volatilisation of combustible gases to vapour phase. On addition of DMP to PA66/NM composite, intumescent effect is observed and the foamed cellular intumescent char layer is formed as seen in **Fig. 6** (iii). The DMP being a source of amine and acid performs as carbonific due to dehydrating action of acid and spumific due to evolution of volatile products. The foamed cellular intumescent char layer formed on the surface acts as a physical barrier that slows heat and mass transfer between the condensed and gas phases and protects the underlying material from the action of the flame as indicated by reduced flame spread rate in UL-94 horizontal test (**Table 4**).

Flammability study (UL-94 test)

UL-94 flammability test is widely used and most frequently cited test for measurement of flammability for plastic materials which includes a standard burning test applied to vertical or horizontal test bars, from which a general flammability rating is derived. In UL-94, the response of a material to a removed fire and its self-extinguishing behaviour are measured. The UL-94 test gives information in a local ignition fire scenario, but their safety level is not so clear when exposed to a more aggressive fire scenario [**24**].

To test the samples in horizontal mode, the polymer strands were marked at 100 mm and time taken (t) by flame to reach this mark was noted as shown in **Table 4**. The flame spread rate was calculated from length of strands and burning time. But the flame spread rate of PA66/NM/DMP is reduced to 1.28 mm/sec from 1.45 mm/sec of PA66. Further a significant reduction in flame spread rate (0.58 mm/sec) is observed on inclusion of APB to PA66/NM/DMP sample having same total loading which indicates the contribution of APB in reducing the flame spread rate even at low loading level of APB (2.5 wt %). The melt dripping behaviour of all composites is reduced than that of pure PA66. The number of flaming drips on formation of composites is decreased. The clay tries to keep the material together. Therefore, flame spread rate is increased as the flame and heat of the material remains bound to the sample. In UL-94 vertical test, no rating was observed for all composites.

Conclusion

PA66/nanoclay nanocomposites were successfully prepared by melt blending method. XRD showed exfoliated structure for PA66/nanoclay nanocomposites at nanoclay loading of 5 wt %. A significant increase in thermal stability was observed after addition of 5 wt % nanoclay to PA66 as indicated by increase in the onset and mid-point temperature of degradation by 25 and 21 °C respectively. The flame retardant (DMP) destabilises the PA66/NM/DMP composite initially but at higher temperature a significant increase in thermal stability and char formation was observed. The addition of APB initially made the thermal degradation of PA66 composite easier due to release of pentaboric acid and later the molten glassy layer of boric acid/boric anhydride accumulated on the surface of composite which helped to regain the thermal stability. The other additives (ZB and KN) provide no contribution to thermal stability and char yield. The DSC data indicated that no significant change in melting point of PA66 is observed on addition of nanomer and other additives. The heat absorbed in PA66 nanocomposites is found to be decreased than pure PA66 indicating that decomposition of the sample is restricted due to formation of nanocomposites. A significant reduction in flame spread rate in UL-94 horizontal test is observed on inclusion of APB to PA66/NM/DMP sample having same total loading. PA66 nanocomposites failed to achieve flame retardant rating in UL-94 vertical test.

Acknowledgements

One of the authors (Sudesh Rathi) is grateful to the Council of Scientific and Industrial Research (CSIR), New Delhi, for the award of Senior Research Fellowship.

Reference

1. Berta, M.; Lindsay, C.; Pans, G.; Camino, G. *Polym. Degrad. Stab.* **2006**, *91*, 1179. **DOI**: 10.1016/j.polymdegradstab.2005.05.027
2. Noh, M.H.; Jang, L.W.; Lee, D.C. *J Appl. Polym. Sci.* **1999**, 74, 179. **DOI**: 10.1002/(SICI)1097-4628(19991003) 74:1<179::AID-APP22>3.0.CO;2-G
3. Zanetti, M.; Camino, G.; Thomann, R.; Mulhaupt, R. *Polymer*. **2001**, 42, 4501. **DOI**: 10.1016/S0032-3861(00)00775-8
4. Goyal, R.K.; Sahu, J.N. *Adv. Mat. Lett.* **2010**, 1, 205. **DOI**: 10.5185/amlett.2010.8151
5. Yuan, X.; Tian, Z. *Adv. Mat. Lett.* **2010**, 1, 135. **DOI**: 10.5185/amlett.2010.4119
6. Qin, H.; Su, Q.; Zhang, S.; Zhao, B.; Yang, M. *Polymer*. **2003**, 44, 7533. **DOI**: 10.1016/j.polymer.2003.09.014
7. Gyoo, P.M.; Venkataramani, S.; Kim, S.C. *J. appl. Polym. Sci.* **2006**, 101, 1711. **DOI**: 10.1002/app.23339
8. Li, Y.; Hu, X. *J. Polym. Sci. Part B: Polym. Phys.* **2007**, 45, 1494. **DOI**: 10.1002/polb.21167
9. Ramesh, C.; Keller, A.; Eltink, S.J.E.A. *Polymer*. **1994**, 35, 2483. **DOI**: 10.1016/0032-3861(94)90367-0
10. Cole, K.C. *Appl Spectrosc*. **2009,** 63, 1343. **DOI**: 10.1366/000370209790108888
11. Charles, J.; Ramkumaar, G.R.; Azhagiri, S.; Gunasekaran, S. *e-J Chem*. **2009,** 6, 23.
12. **DOI**:10.1155/2009/909017
13. Madejova, J. *Vib. Spectrosc.* **2003**, 31, 1. **DOI**: 10.1016/S0924-2031(02)00065-6
14. Patel, H.A.; Somani, R.S.; Bajaj, H.C.; Jasra, R.V. *Ind. Eng. Chem. Res*. **2010**, 49, 1677. **DOI:** 10.1021/ie801368b
15. Xi, Y.; Ding, Z.; He, H.; Frost, R.L. *Spectrochim. Acta. Part A.* **2005**, 61, 515. **DOI**: 10.1016/j.saa.2004.05.001
16. Levchik, S.V.; Weil, E.D.; Lewin, M. *Polym. Int*. **1999**, 48, 532. **DOI**:10.1002/(SICI)1097-0126(199907)48:7<532::AID-PI214>3.0.CO;2-R
17. Levchik, S.V.; Costa, L.; Camino, G. *Polym. Degrad. Stab*. **1992**, 36, 31. **DOI**: 10.1016/0141-3910(92)90045-7
18. Levchik, S.V.; Costa, L.; Camino, G. *Polym. Degrad. Stab*. **1994**, 43, 43. **DOI**: 10.1016/0141-3910(94)90224-0
19. Araujo, E.M.; Barbosa, R.; Rodrigues, A.W.B.; Melo, T.J.A.; Ito, E.N. *Mater. Sci. Eng. A*, **2007,** 445-446, 141. **DOI**: 10.1016/j.msea.2006.09.012
20. Zhao, C.; Qin, H.; Gong, F.; Feng, M.; Zhang, S.; Yang, M. *Polym. Degrad. Stab.* **2005,** 87, 183**.** **DOI**: 10.1016/j.polymdegradstab.2004.08.005
21. Levchik, S. V.; Balabanovich, A. I.; Levchik, G. F.; Costa, L. *Fire Mater*. **1997**, 21, 75. **DOI**:10.1002/(SICI)1099-1018(199703)21:2<75::AID-FAM597>3.0.CO;2-P
22. Gilman, J.W. *Appl. Clay. Sci.* **1999**, 15, 31. **DOI**: 10.1016/S0169-1317(99)00019-8
23. Levchik, S.V.; Balabanovich, A.I.; Levchik, G.F.; Camino, G.; Costa, L. *Polym. Degrad. Stab*. **1996**, 54, 217. **DOI**: 10.1016/S0141-3910(96)00046-8
24. Erdey, L.; Gal, S.; Liptay, G. *Talanta*. **1964**, 11, 913. **DOI**: 10.1016/0039-9140(64)80128-4
25. Morgan, A.B.; Bundy, M. *Fire Mater.* **2007**, 31, 257. **DOI**: 10.1002/fam.937

